Title: Interplay between Desmoglein2 and hypoxia controls intravasation and circulating tumor cell clustering in breast cancer metastasis

Author Affiliation: Po-Hao Chang[1], Min-Che Chen[2], Ya-Ping Tsai[2], Pang-Hung Hsu[3], Yung-Ming Jeng[4], Wendy W. Hwang-Verslues[1,*]

[1]Genomics Research Center, Academia Sinica, No. 128, Sec. 2, Academia Road, Taipei 115, Taiwan

[2]Asclepiumm Taiwan Co., Ltd, Mackay Memorial Hospital Innovation & Incubation Center, No. 45, Minsheng Rd, Tamsui, New Taipei City 25160, Taiwan

[3]Department of Bioscience and Biotechnology, National Taiwan Ocean University, No.2, Beining Rd., Jhongjheng District, Keelung City 20224, Taiwan

[4]Department of Pathology, National Taiwan University Hospital, No.7, Chung Shan S. Rd., Zhongzheng Dist., Taipei 100, Taiwan

Corresponding Author*: Wendy W. Hwang-Verslues, Ph.D., Genomics Research Center, Academia Sinica, No. 128, Sec. 2, Academia Road, Taipei 115, Taiwan. **Email:** wendyhv@gate.sinica.edu.tw, **Phone:** +886-2-2787-1246, **Fax:** +886-2-2789-9924, **ORCID:** 0000-0002-0383-1710

Keywords: Desmoglein2 (DSG2), breast cancer, hypoxia, HIF1α, circulating tumor cells (CTCs), metastasis

Abstract

Interaction between tumor cells and their microenvironment plays a critical role in tumorigenesis and metastasis. Disseminated tumor cells in the blood (circulating tumor cells (CTCs)), particularly CTC clusters, are positively correlated with metastatic potential and poor prognosis. However, the key factors required for tumor cell dissemination and CTC clustering remain elusive. We found that Desmoglein2 (DSG2), a key cell adhesion molecule participated in desmosome mediated intercellular adhesion, and its regulation by hypoxia, a potent microenvironmental factor linked to cancer progression, were critical for breast tumorigenesis, CTC clustering and metastasis. Expression of DSG2 was positively correlated with poor prognosis and recurrence risk in breast cancer patients. High DSG2 expression promoted tumor growth, CTC clustering and distant organ colonization. Conversely, epithelial-to-mesenchymal transition (EMT), invasion and intravasation were able to occur when DSG2 was suppressed under hypoxia. In hypoxic cancer cells, HIF1α directly bound and recruited polycomb repressive complex 2 components to the DSG2 proximal promoter, thus allowing cells to detach from the primary tumor. Once hypoxic stress was released in the vascular system, DSG2 de-repression allowed CTCs to form clusters and colonize in distant organs. Together, our results demonstrated the role of DSG2 expression in breast tumor progression and cancer metastasis. These data also revealed a new molecular mechanism by which hypoxia drives metastasis.

Significant Statement

During metastasis, a hypoxic microenvironment is a major force driving primary tumor cells to disseminate into the circulatory system. The majority of these circulating tumor cells (CTCs) cannot survive when traveling alone. However, collective movement as CTC clusters enables them to avoid immune surveillance and increases the probability that they will successfully metastasize to distal organs. Dynamic down regulation of DSG2 in hypoxic tumor tissue and reactivation of expression in CTCs allowed high rates of tumor cell dissemination, CTC cluster formation and metastasis that are characteristics of the most aggressive breast cancers. The findings highlight both the potential, and potential pitfalls, of using DSG2 as a therapeutic target.

Introduction

Breast cancer is the most common cancer of women worldwide. With early detection and advance in therapeutic strategies, the 5-year relative survival rate for all stages combined is higher than 90% (according to the SEER database maintained by the U.S. National Cancer Institute). However, metastasis is now the major cause of breast cancer death (1) as the survival rate for women with metastasized breast cancers remains below 30%. Thus, identification of key factors in breast tumorigenesis and metastasis is important to identify therapeutic targets and strategies to improve prognosis.

Metastasis is a complex process involving tumor cell intrinsic alterations and extrinsic interaction with the microenvironment to select for highly aggressive cancer cells. Hypoxia, a key microenvironmental factor in solid tumors, activates hypoxic signaling in tumor cells to increase cell plasticity by promoting epithelial-to-mesenchymal transition (EMT) to drive the first step of metastasis (2). High plasticity allows these cancer cells to disseminate from the primary site and intravasate into circulatory or lymphatic system. Most of these circulating tumor cells (CTCs) die in circulation and only a small fraction of CTCs are able to survive and eventually colonize at distant organs (3, 4). Recent evidence has shown that CTC numbers can be used as an independent predictor for survival in patients with metastatic cancers (5-7). With continuous improvement in

CTC detection methods, CTC clusters were identified. Evidence has shown that CTCs in the clusters exhibit epithelial/mesenchymal hybrid (partial EMT) phenotype which allows them to move collectively (8). Collective movement makes these cancer cells to be more apoptosis-resistant and more capable of avoiding immune surveillance and colonizing distant organs. Importantly, the clustering ability of these cancer cells was positively correlated with poor clinical outcome (9-12). However, the factors that drive CTC cluster forming and how these clusters promote metastasis remain elusive.

Cell adhesion proteins play critical roles in intercellular contacts and epithelial tissue dynamics. Deregulation of cell adhesion molecules contributes to tumor metastasis (13, 14). Among cell adhesion molecules, desmosomes are of particular interest for cancer biology. Desmosomes form patch-like adhesion structures that mark the intercellular midline and connect to the intermediate filament cytoskeleton to maintain cell-cell adhesion and tissue integrity (15). The desmosome is a protein complex containing two transmembrane proteins, Desmocollin (DSC1-DSC3) and Desmoglein (DSG1-DSG4), as well as adaptor proteins, Plakoglobin and Desmoplakin, that bind intermediate filaments (16). Among the DSGs, DSG2 is the most ubiquitously expressed isoform in many tissues, including mammary, and is a key factor for cell aggregation and oncogenic function in lung and prostate cancers (17-20). However, the role of DSG2 in CTC clustering and metastasis

remains uncharacterized.

We found that breast cancer patients whose tumors had high DSG2 expression (DSG2-high) had worse prognosis and higher recurrence risk than those with DSG2-low tumors. DSG2 expression enhanced CTC clustering and facilitated metastasis. Tumor growth and colonization were also promoted by DSG2 expression at both the primary site and distant organ. However, suppression of DSG2 mediated by HIF1α under hypoxia was required for intravasation. Once in the circulatory system, the cancer cells were released from hypoxic stress and DSG2 expression was de-repressed. This reactivation of DSG2 was essential for formation of CTC clusters and colonization of distant organs. Together, these results show that dynamic changes of DSG2 expression are required for breast tumorigenesis, intravasation, CTC clustering and metastasis. Our data also identify regulatory mechanisms underlying DSG2 repression and de-repression during specific stages of breast cancer progression.

Result

High expression of DSG2 in breast cancer is associated with poor prognosis and high recurrence

To identify key factors driving CTC clustering and metastasis, we analyzed a transcriptome dataset for metastatic and non-metastatic breast cancers from the Gene Expression Omnibus (GEO)

of the National Center for Biotechnology Information using Gene Set Enrichment Analysis (GSEA). Forty-six genes associated with metastatic disease were enriched in metastatic breast cancers. Among these, DSG2 was the most highly expressed (Fig. 1, A and B). Because formation of CTC clusters (groups of two or more aggregated CTCs) promotes metastasis and because cell-cell interaction is critical for CTC clustering (9), we also analyzed genes associated with cell-cell junctions and found DSG2 as the second highly expressed gene among 56 genes enriched in the metastatic group (*SI Appendix*, Fig. S1A and B). Overlap of these two gene sets (metastasis and cell-cell junction) identified three genes (*SI Appendix*, Fig. 1C). Among these, DSG2 was the gene most highly upregulated in the metastasis and cell-cell junction gene sets enriched in the metastatic breast cancer patients.

We then evaluated clinical correlation of DSG2 expression with prognosis using immunohistochemistry (IHC) analysis of 164 biopsy specimens (Fig. 1C). Based on the IHC analysis, patients were grouped into “DSG2-high” and “DSG2-low” groups for Kaplan–Meier survival analyses. The disease-free survival was significantly lower in the DSG2-high group (Fig. 1D, $p = 0.004$). Importantly, DSG2 expression was highly correlated with cancer recurrence (Fig. 1E, $p = 0.03$). To examine whether high DSG2 expression promoted metastasis, we analyzed a breast cancer cohort from the UCSC Xena public hub (Yau 2010 dataset)(21) and found significantly

lower distant metastasis-free survival in DSG2-high breast cancer patients (Fig. 1F, $p = 0.008$). The results from these three independent cohorts indicated that DSG2 possesses a metastatic role in breast cancer and can be used as a prognostic marker.

DSG2 expression promotes CTC clustering and facilitates metastasis

To determine DSG2 function in breast cancer progression, we first examined endogenous DSG2 levels in a panel of cell lines (*SI Appendix*, Fig. 2A). MDA-MB-231, a model cell line for *in vivo* metastasis studies due to its high metastatic potential (22), was found to express the highest level of DSG2. MDA-MB-231 was then used for loss-of-function experiments where DSG2 expression was depleted using a lentiviral-shRNA system (*SI Appendix*, Fig. 2B). Depletion of DSG2 on the cell membrane was confirmed by fluorescence activated cell sorting (FACS) (*SI Appendix*, Fig. 2C). To investigate the role of DSG2 in CTC clustering and metastasis, orthotopic xenograft assay was performed by injecting EGFP expressing MDA-MB-231 cells, without (shCtrl) or with (shDSG2) DSG2 depletion, into the 4th mammary fat-pad of NOD/SCIDγ mice. Nine weeks after mammary fat pad injection, tumor size, CTC counts and lung nodules were evaluated (Fig. 2A). Tumors derived from shCtrl cells were bigger (Fig. 2B) and these mice had more metastatic nodules in the lungs compared to the mice bearing shDSG2 cell-derived tumors (Fig. 2C). Moreover, IHC staining confirmed that the cells which colonized and formed nodules in the lungs expressed DSG2

(Fig. 2D). Using a CTC platform (MiCareo), we observed that not only were there more CTCs detected in the shCtrl group, but also the majority of the CTCs collected from the shCtrl group were clustered (Fig. 2, E and F). In contrast, shDSG2 had a 5-fold lower prevalence of CTC clusters (278 clusters per gram tumor in the shCtrl group, 59 clusters per gram tumor in the shDSG2 group). These data indicated that DSG2 facilitates breast cancer metastasis and also promotes CTC clustering.

DSG2 expression promotes metastatic colonization and tumor growth

As colonization is a crucial step to determine whether cancer cells can survive in distant organs (23, 24), we injected SKBR3 cells, which also had high levels of endogenous DSG2 expression (*SI Appendix*, Fig. 2A), with or without DSG2 depletion into mouse tail vein to examine whether DSG2 contributes to colonization ability. Fixation and hematoxylin and eosin (H&E) staining of lung tissue two months after the initial tail vein injection showed that mice injected with DSG2-depleted SKBR3 cells had significantly lower numbers of lung nodules compared to mice injected with control cells (Fig. 3, A and B). Conversely, DSG2 overexpression in MDA-MB-157 cells, which had low levels of endogenous DSG2 expression (*SI Appendix*, Fig. 2A), significantly increased lung colonization by cells (Fig. 3, C and D).

In addition, DSG2 promoted tumor growth at the primary site. DSG2 depletion led to

significant reduction of colony forming efficiency in soft agar colony forming (SACF) assays (Fig. 3E). Conversely, DSG2 overexpression in MDA-MB-157 and MDA-MB-468 cells, which had low endogenous DSG2 levels (*SI Appendix*, Fig. 2, A-C), resulted in higher colony numbers (Fig. 3F). Consistent with the tumorigenic role of DSG2 in promoting colony formation, orthotopic xenografts showed that tumors derived from DSG2-depleted cancer cells were significantly smaller than the control while cells overexpressing DSG2 formed significantly larger tumors (Fig. 3, G and H, and *SI Appendix*, Fig. 2, D and E). Together, these results demonstrated that DSG2 expression promotes breast tumor growth at the primary site and increases colonization in the distal organs.

DSG2 has been reported to participate in cell adhesion through its interaction with another desmosome component, DSC2, and to activate EGFR signaling to promote tumor growth (20, 25, 26). Since not every DSG2-expressing cell line expressed DSC2 or EGFR (*SI Appendix*, Fig. 3A), we sought to identify other DSG2-interacting proteins contributing to DSG2-mediated tumorigenesis and colonization. Immunoprecipitation followed by liquid chromatography-tandem mass spectrometry (LC-MS/MS) found β-Actin (ACTB) as one of the top candidates among putative DSG2-interactors identified (*SI Appendix*, Fig. 3B). DSG2-ACTB interaction was confirmed by Co-IP (*SI Appendix*, Fig. 3C). DSG2 interaction with ACTB may be mediated by Plakoglobin (γ -catenin) or Plakophilin, members of the Armadillo protein family that bind DSG2 and the actin

cytoskeleton (15, 27). Importantly, while β-Actin protein level was slightly reduced in DSG2-depleted cells, it was strongly elevated upon DSG2 overexpression (*SI Appendix*, Fig. 3D). This result was consistent with DSG2 promotion of metastasis as increase in β-Actin expression has been particularly implicated in metastatic cancers (28-30).

Moreover, dynamic assembly and disassembly of microfilaments (filamentous (F)-Actin) from G-actin monomers is generally important in cell integrity and control of mobility (31) and specifically important for the establishment of a circumferential F-actin belt parallel to the cell-cell contact area (32). Such microfilament structure is regulated by RhoA GTPase to control membrane rigidity and prevent anchorage detachment (33, 34). We found that RhoA activity was decreased upon DSG2 suppression but increased when DSG2 was ectopically expressed (*SI Appendix*, Fig. 3E). This result was consistent with the observation that Rho GTPases participated in desmosomal cadherin-mediated cell adhesion (35). We also observed a dramatic decrease in F-Actin (visualized using phalloidin) in DSG2-depleted cells (*SI Appendix*, Fig. 3F). Conversely, ectopic expression of DSG2 significantly increased F-actin (*SI Appendix*, Fig. 3G). Together, these data suggested that DSG2 promotion of anchorage independent growth and CTC clustering may be mediated, at least in part, by β-actin-controlled cell junction integrity and remodeling.

DSG2 expression inhibits cell invasion, migration and intravasation by decreasing EMT genes

Initiation of cancer metastasis, including invasion, migration and intravasation, relies heavily on tumor cell dissemination (1, 36). Since DSG2 expression increased CTC clustering and tumor growth in the mammary fat pad and also promoted colonization in the lung, we next evaluated its role in dissemination. Seemingly in contrast to its tumorigenic role, DSG2 knockdown in MDA-MB-231 cells significantly increased migration ability (Fig. 4A) and DSG2 overexpression in MDA-MB-157 cells inhibited migration (Fig. 4B). Similarly, depletion of DSG2 increased cell invasion; whereas overexpression of DSG2 inhibited this ability (Fig. 4, C and D). Consistent with these observations, DSG2 depletion resulted in an upregulation of EMT genes, including *SNAIL*, *SLUG* and *VIMENTIN*, all of which are critical for cancer cell mobility and dissemination (37, 38). Conversely, DSG2 overexpression downregulated these genes (*SI Appendix*, Fig. 4). Together these findings indicated that suppression of DSG2 facilitates invasion and migration not only by disruption of cell-cell adhesion but also by upregulation of EMT genes.

We next examined whether DSG2 depletion promotes intravasation *in vivo* using orthotopic xenograft model. Five weeks after injection of EGFP expressing MDA-MB-231 cells transduced with shDSG2 or shCtrl, FACS detection of CTCs in blood samples found higher CTC numbers in mice xenografted with DSG2-depleted cells than in the control (Fig. 4E). These results demonstrated that DSG2 suppression promotes cell migration, invasion and intravasation into the

circulatory system.

Intriguingly, blood samples collected 8-weeks after injection of shCtrl MDA-MB-231 contained CTC numbers just as high as those mice injected with DSG2-depleted cells (Fig. 4F). This result indicated that from 5-8 weeks after injection, tumors derived from the shCtrl MDA-MB-231 cells underwent some alteration that increased intravasation ability. Interestingly, at 8 weeks after injection, tumors derived from the shCtrl MDA-MB-231 cells had high DSG2 in the tumor boundary but low DSG2 in the tumor central region (Fig. 4G). This DSG2 expression pattern was opposite to intra-tumor hypoxia gradient (high in the center but low in the boundary) (39) and indicated that DSG2 expression may be downregulated by hypoxia. Consistent with this hypothesis, we found a negative correlation between expression of DSG2 and CAIX, a hypoxic stress marker, in tumor sections from the mouse xenograft model (Fig. 4H). This inverse correlation was also observed in clinical specimens where it was observed that regions with high DSG2 expression had low CAIX expression and *vice versa* (Fig. 4I).

Hypoxia-induced HIF1α suppresses DSG2 expression

Hypoxia plays a critical role in metastasis (2) but it is not known whether hypoxia affects DSG2 suppression during tumor progression. Consistent with the pattern of DSG2 expression in tumor specimens, breast cancer cells subjected to hypoxic stress had decreased DSG2 gene expression and

protein level (Fig. 5, A and B). Similarly, DSG2 expression decreased in cells treated with different doses or durations of the hypoxia-mimetic agent $CoCl_2$ (*SI Appendix*, Fig. 5, A and B). Since HIF1α is a critical mediator of hypoxia-associated cancer progression (40), we determined the effect of HIF1α on DSG2 expression. Transient transfection of a non-degradable HIF1α (P564A) in HEK-293T cells resulted in downregulation of DSG2 (Fig. 5C). Importantly, depletion of HIF1α in HEK-293T treated with $CoCl_2$ abolished hypoxia-induced DSG2 suppression (Fig. 5D). These results indicated that HIF1α is responsible for DSG2 suppression under hypoxic stress.

To further elucidate whether HIF1α directly suppressed DSG2 transcription, we used Integrated Motif Activity Response Analysis (ISMAR) (41) to identify putative HIF1α binding sites and found that mutation of one of these sites (-946 to -943) abolished HIF1α inhibition of DSG2 expression (Fig. 5E). Chromatin-immunoprecipitation (ChIP) further confirmed that hypoxia-induced HIF1α bound to this region (Fig. 5F and *SI Appendix*, Fig. 5C). To understand how HIF1α carried out this transcriptional suppression, we performed Co-IP assays and found HIF1α interaction with polycomb repressive complex 2 components, EZH2 and SUZ12, but not HDAC1 and HDAC2, in breast cancer cells under hypoxia (*SI Appendix*, Fig. 5, D and E). Upon hypoxic stress, these co-repressors associated with the HIF1α-binding region on the DSG2 promoter leading to an increase in H3K27-trimethylation (H3K27me3) indicative of heterochromatin formation (Fig. 5G). Together,

these results indicated that HIF1α recruits PRC2 complex to the DSG2 promoter to suppress its transcription under hypoxic stress.

Since DSG2 is critical for distant organ colonization and expressed in metastatic nodules (Fig. 2 and Fig. 3), DSG2 suppression that occurs in hypoxic conditions must be released before colonization can occur. Consistent with this idea, de-repression of DSG2 expression was observed after breast cancer cells were released from hypoxia *in vitro* (Fig. 5H). To confirm that this reactivation is important *in vivo*, we injected EGFP expressing MDA-MB-231 cells into mammary fat pads and evaluated DSG2 expression in CTCs after injection. Before injection, nearly all cells expressed DSG2 (98.6%, Fig. 5I). At nine weeks after injection, more than 90% of CTCs disseminated from the primary tumor site expressed DSG2 while 9% had low/non-detectable DSG2, possibly indicating that they had just been released from the primary tumor and undergone intravasation (Fig. 5I). These data indicated that hypoxia-mediated DSG2 suppression followed by de-repression of DSG2 when hypoxic stress is released in the circulatory system is required for DSG2-promoted breast cancer metastasis.

Discussion

Our study demonstrated that dynamic changes in DSG2 expression are important for breast tumorigenesis and malignancy (Fig. 6). High DSG2 expression facilitated breast tumor growth in

mammary tissue, CTC clustering in blood and colonization in lung. However, downregulation of DSG2 was critical for intravasation. In addition to the clinical implications of these results, we also mark out clear avenues to further establish the molecular basis of DSG2 function in cancer progression. Unlike in colon cancer where DSG2 interacted with EGFR and AKT/β-catenin signaling to promote cancer cell proliferation (26, 42), DSG2 promoted breast tumor growth by elevating anchorage-independent growth ability. This may be associated with Rho A/β-actin controlled cell junction formation. Interestingly, the actin cytoskeleton has previously been implicated in CTC stabilization and dissemination (43). Our results further demonstrated that DSG2 overexpression could promote tumorigenesis in MDA-MB-157 and SKBR3 cells even though MDA-MB-157 cells do not express DSC2, and neither MDA-MB-157 nor SKBR3 express EGFR (*SI Appendix*, Fig. 3A). Thus, there are likely to be other, yet unidentified, DSG2 interacting transmembrane proteins critical for DSG2-mediated tumorigenic activity. Furthermore, the correlation between DSG2 expression and β-Actin protein level as well as EMT gene expression is also intriguing. In normal epithelial cells, cytoplasmic β-Actin and γ-Actin, are both expressed (44); however, β-Actin specifically controls the steady-state adhesion junction integrity, is required for apico-basal cell polarity and, cooperates with γ-Actin to from three-dimensional epithelial cysts (45). All of these functions are consistent with DSG2-mediated changes in adhesion during tumorigenesis

and colonization. Whether high DSG2 expression affects microfilament stability via DSG2-associated actin binding proteins and how perturbed DSG2 expression dysregulates β-Actin and EMT gene expression remain to be elucidated.

Consistent with our observations that DSG2 expression promoted CTC clustering (Fig. 2), Plakoglobin (γ -catenin), a member of the Armadillo family proteins that binds DSG2 and the actin cytoskeleton, has also been shown to contribute to CTC cluster formation and cancer metastasis (9, 46). Moreover, CTCs that can survive in the circulatory system and colonize in distant organs are thought to be cancer stem-like cells and are highly correlated with metastasis (47, 48). Consistent with this notion, DSG2 has recently been identified as a marker for pluripotent stem cells (PSCs) and is critical for PSC self-renewal and reprogramming (49). How DSG2 may contribute to cancer stemness is another topic of interest for further experiments.

Our clinical data and animal models clearly demonstrated that DSG2 can be used as a prognostic marker for breast cancer. Interestingly, DSG2 expression is also associated with poor prognosis in other cancers including cervical, head and neck and lung cancers (*SI Appendix*, Fig. 6). This suggests a widespread role of DSG2 in cancer malignancy. As a transmembrane protein, DSG2 may be a drugable target. However, the strategy has to be carefully designed. Using a monoclonal DSG2 specific antibody to target the DSG2 to inhibit anchorage independent growth

may be possible. However, antibody-DSG2 internalization may occur and result in enhancement of intravasation, as downregulation of DSG2 promotes invasion. In this case, a well-designed antibody-cytotoxic drug conjugate (ADC) (50) may be a more effective therapeutic method to target DSG2 expressing cancer cells. In addition, since DSG2 expressing CTCs tend to form clusters which facilitate distant organ colonization, dialysis for DSG2 expressing cancer cells in the blood may be another way to inhibit metastasis. Overall, the underlying molecular mechanisms of DSG2-mediated tumorigenesis and the possibility of using DSG2 as a cancer therapeutic target warrant further studies.

Materials and Methods

Cell lines and cell culture

Cancer cell lines including MDA-MB-231, MDA-MB-157, MDA-MB-468, and SKBR3 were obtained from the American Type Culture Collection. Cells were maintained in DMEM supplemented with 10% fetal bovine serum and antibiotics and cultured at 37°C in a humidified incubator supplemented with 5% CO_2. For hypoxia experiments, medium was first incubated in HypoxyCOOL system (Baker) for 8 hours to reduce oxygen level to 1%. This medium was then used to culture the cells in INVIVO 400 hypoxia chamber (Baker) supplemented with 5% CO_2 and 1% O_2 at 37°C. Further details of experimental methods are given in the *SI Appendix*, Materials and Methods.

Author contributions

P.-H.C. and W.W.H.-V. conceived the paper. P.-H.C. performed the experiments. P.-H.H. assisted with the LC-MS/MS analysis and Y.-M.J. assisted with immunohistochemistry analysis, P.-H.C. and P.-H.H. analyzed the data, M.-C.C. and Y.-P.T. generated the DSG2 antibody. P.-H.C. and W.W.H.-V. wrote the paper.

Acknowledgements

This work was supported by Academia Sinica [AS-SUMMIT-108] and Ministry of Science and Technology [MOST 108-3114-Y-001-002] and/or [MOST 107-0210-01-19-01and [MOST 105-2628-B-001-008-MY3]. The authors would like to thank Dr. Michael Hsiao (Genomics Research Center, Academia Sinica, Taiwan) for providing NOD/SCID mice, and Dr Yi-Cheng Chang

(Graduate Institute of Medical Genomics and Proteomics, National Taiwan University) for discussion.

Reference

1. C. L. Chaffer, R. A. Weinberg, A perspective on cancer cell metastasis. *Science* **331**, 1559-1564 (2011).

2. E. B. Rankin, A. J. Giaccia, Hypoxic control of metastasis. *Science* **352**, 175-180 (2016).

3. J. D. Twomey, B. Zhang, Circulating Tumor Cells Develop Resistance to TRAIL-Induced Apoptosis Through Autophagic Removal of Death Receptor 5: Evidence from an In Vitro Model. *Cancers (Basel)* **11** (2019).

4. P. A. Theodoropoulos *et al.*, Circulating tumor cells with a putative stem cell phenotype in peripheral blood of patients with breast cancer. *Cancer Lett* **288**, 99-106 (2010).

5. S. J. Cohen *et al.*, Relationship of circulating tumor cells to tumor response, progression-free survival, and overall survival in patients with metastatic colorectal cancer. *J Clin Oncol* **26**, 3213-3221 (2008).

6. M. Cristofanilli *et al.*, Circulating tumor cells, disease progression, and survival in metastatic breast cancer. *N Engl J Med* **351**, 781-791 (2004).

7. J. S. de Bono *et al.*, Circulating tumor cells predict survival benefit from treatment in metastatic castration-resistant prostate cancer. *Clin Cancer Res* **14**, 6302-6309 (2008).

8. X. Liu *et al.*, Epithelial-type systemic breast carcinoma cells with a restricted mesenchymal transition are a major source of metastasis. *Sci Adv* **5**, eaav4275 (2019).

9. N. Aceto *et al.*, Circulating tumor cell clusters are oligoclonal precursors of breast cancer metastasis. *Cell* **158**, 1110-1122 (2014).

10. E. H. Cho *et al.*, Characterization of circulating tumor cell aggregates identified in patients with epithelial tumors. *Phys Biol* **9**, 016001 (2012).

11. J. M. Hou *et al.*, Clinical significance and molecular characteristics of circulating tumor cells and circulating tumor microemboli in patients with small-cell lung cancer. *J Clin Oncol* **30**, 525-532 (2012).

12. Z. Mu *et al.*, Prospective assessment of the prognostic value of circulating tumor cells and their clusters in patients with advanced-stage breast cancer. *Breast Cancer Res Treat* **154**, 563-571 (2015).

13. A. Eger, A. Stockinger, B. Schaffhauser, H. Beug, R. Foisner, Epithelial mesenchymal transition by c-Fos estrogen receptor activation involves nuclear translocation of beta-catenin and upregulation of beta-catenin/lymphoid enhancer binding factor-1 transcriptional activity. *J Cell Biol* **148**, 173-188 (2000).

14. T. T. Onder *et al.*, Loss of E-cadherin promotes metastasis via multiple downstream

transcriptional pathways. *Cancer Res* **68**, 3645-3654 (2008).

15. D. Garrod, M. Chidgey, Desmosome structure, composition and function. *Biochim Biophys Acta* **1778**, 572-587 (2008).

16. E. Delva, D. K. Tucker, A. P. Kowalczyk, The desmosome. *Cold Spring Harb Perspect Biol* **1**, a002543 (2009).

17. S. Schafer, P. J. Koch, W. W. Franke, Identification of the ubiquitous human desmoglein, Dsg2, and the expression catalogue of the desmoglein subfamily of desmosomal cadherins. *Exp Cell Res* **211**, 391-399 (1994).

18. F. Cai *et al.*, Desmoglein-2 is overexpressed in non-small cell lung cancer tissues and its knockdown suppresses NSCLC growth by regulation of p27 and CDK2. *J Cancer Res Clin Oncol* **143**, 59-69 (2017).

19. A. G. Barber *et al.*, Characterization of desmoglein expression in the normal prostatic gland. Desmoglein 2 is an independent prognostic factor for aggressive prostate cancer. *PLoS One* **9**, e98786 (2014).

20. L. Saias, A. Gomes, M. Cazales, B. Ducommun, V. Lobjois, Cell-Cell Adhesion and Cytoskeleton Tension Oppose Each Other in Regulating Tumor Cell Aggregation. *Cancer Res* **75**, 2426-2433 (2015).

21. B. C. Mary Goldman, Mim Hastie, Kristupas Repečka, Akhil Kamath, Fran McDade, Dave Rogers, Angela N Brooks, Jingchun Zhu, David Haussler (The UCSC Xena platform for public and private cancer genomics data visualization and interpretation. in *bioRxiv 326470*.

22. J. E. Price, A. Polyzos, R. D. Zhang, L. M. Daniels, Tumorigenicity and metastasis of human breast carcinoma cell lines in nude mice. *Cancer Res* **50**, 717-721 (1990).

23. J. Massague, A. C. Obenauf, Metastatic colonization by circulating tumour cells. *Nature* **529**, 298-306 (2016).

24. D. X. Nguyen, P. D. Bos, J. Massague, Metastasis: from dissemination to organ-specific colonization. *Nat Rev Cancer* **9**, 274-284 (2009).

25. O. J. Harrison *et al.*, Structural basis of adhesive binding by desmocollins and desmogleins. *Proc Natl Acad Sci U S A* **113**, 7160-7165 (2016).

26. R. Kamekura *et al.*, Loss of the desmosomal cadherin desmoglein-2 suppresses colon cancer cell proliferation through EGFR signaling. *Oncogene* **33**, 4531-4536 (2014).

27. M. Hatzfeld, C. Haffner, K. Schulze, U. Vinzens, The function of plakophilin 1 in desmosome assembly and actin filament organization. *J Cell Biol* **149**, 209-222 (2000).

28. A. Popow, D. Nowak, M. Malicka-Blaszkiewicz, Actin cytoskeleton and beta-actin expression in correlation with higher invasiveness of selected hepatoma Morris 5123 cells. *J*

Physiol Pharmacol **57 Suppl 7**, 111-123 (2006).

29. D. Nowak, A. Skwarek-Maruszewska, M. Zemanek-Zboch, M. Malicka-Blaszkiewicz, Beta-actin in human colon adenocarcinoma cell lines with different metastatic potential. *Acta Biochim Pol* **52**, 461-468 (2005).

30. P. U. Le, T. N. Nguyen, P. Drolet-Savoie, N. Leclerc, I. R. Nabi, Increased beta-actin expression in an invasive moloney sarcoma virus-transformed MDCK cell variant concentrates to the tips of multiple pseudopodia. *Cancer Res* **58**, 1631-1635 (1998).

31. A. I. Bachir, A. R. Horwitz, W. J. Nelson, J. M. Bianchini, Actin-Based Adhesion Modules Mediate Cell Interactions with the Extracellular Matrix and Neighboring Cells. *Cold Spring Harb Perspect Biol* **9** (2017).

32. M. K. Hoelzle, T. Svitkina, The cytoskeletal mechanisms of cell-cell junction formation in endothelial cells. *Mol Biol Cell* **23**, 310-323 (2012).

33. M. Bezanilla, A. S. Gladfelter, D. R. Kovar, W. L. Lee, Cytoskeletal dynamics: a view from the membrane. *J Cell Biol* **209**, 329-337 (2015).

34. T. Dorn *et al.*, Interplay of cell-cell contacts and RhoA/MRTF-A signaling regulates cardiomyocyte identity. *EMBO J* **37** (2018).

35. V. Spindler, J. Waschke, Role of Rho GTPases in desmosomal adhesion and pemphigus

pathogenesis. *Ann Anat* **193**, 177-180 (2011).

36. D. R. Welch, D. R. Hurst, Defining the Hallmarks of Metastasis. *Cancer Res* **79**, 3011-3027 (2019).

37. M. A. Nieto, Context-specific roles of EMT programmes in cancer cell dissemination. *Nat Cell Biol* **19**, 416-418 (2017).

38. A. Barrallo-Gimeno, M. A. Nieto, The Snail genes as inducers of cell movement and survival: implications in development and cancer. *Development* **132**, 3151-3161 (2005).

39. H. J. Knox *et al.*, A bioreducible N-oxide-based probe for photoacoustic imaging of hypoxia. *Nat Commun* **8**, 1794 (2017).

40. A. L. Harris, Hypoxia--a key regulatory factor in tumour growth. *Nat Rev Cancer* **2**, 38-47 (2002).

41. P. J. Balwierz *et al.*, ISMARA: automated modeling of genomic signals as a democracy of regulatory motifs. *Genome Res* **24**, 869-884 (2014).

42. K. Kolegraff, P. Nava, M. N. Helms, C. A. Parkos, A. Nusrat, Loss of desmocollin-2 confers a tumorigenic phenotype to colonic epithelial cells through activation of Akt/beta-catenin signaling. *Mol Biol Cell* **22**, 1121-1134 (2011).

43. M. A. Matrone, R. A. Whipple, E. M. Balzer, S. S. Martin, Microtentacles tip the balance of

cytoskeletal forces in circulating tumor cells. *Cancer Res* **70**, 7737-7741 (2010).

44. T. M. Bunnell, B. J. Burbach, Y. Shimizu, J. M. Ervasti, beta-Actin specifically controls cell growth, migration, and the G-actin pool. *Mol Biol Cell* **22**, 4047-4058 (2011).

45. S. Baranwal *et al.*, Nonredundant roles of cytoplasmic beta- and gamma-actin isoforms in regulation of epithelial apical junctions. *Mol Biol Cell* **23**, 3542-3553 (2012).

46. C. A. Gaudry *et al.*, Tyrosine-phosphorylated plakoglobin is associated with desmogleins but not desmoplakin after epidermal growth factor receptor activation. *J Biol Chem* **276**, 24871-24880 (2001).

47. V. Plaks, C. D. Koopman, Z. Werb, Cancer. Circulating tumor cells. *Science* **341**, 1186-1188 (2013).

48. S. A. Joosse, T. M. Gorges, K. Pantel, Biology, detection, and clinical implications of circulating tumor cells. *EMBO Mol Med* **7**, 1-11 (2015).

49. J. Park *et al.*, DSG2 Is a Functional Cell Surface Marker for Identification and Isolation of Human Pluripotent Stem Cells. *Stem Cell Reports* **11**, 115-127 (2018).

50. J. Y. Li *et al.*, A Biparatopic HER2-Targeting Antibody-Drug Conjugate Induces Tumor Regression in Primary Models Refractory to or Ineligible for HER2-Targeted Therapy. *Cancer Cell* **29**, 117-129 (2016).

Figure Legends

Figure 1. High DSG2 expression is positively correlated with metastasis and high recurrence risk in breast cancer patients.

(A, B) GSEA-P enrichment plot (A) and heat map (B) for the top 30 up-regulated genes for metastasis in metastatic (n = 7) versus non-metastatic breast cancer patients (n = 15). Normalized enrichment score (NES) and FDR q are listed on the enrichment plots. (C) Representative immunohistochemistry (IHC) of breast tumors with low (upper panel) and high (lower panel) DSG2 expression. Enlarged images are presented on the right. Scale bar, 30 μm. (D) Kaplan-Meier disease free survival analysis of breast cancer patients grouped by DSG2 expression. DSG2-high group is indicated by red line (n = 113); DSG2-low group is indicated by black line (n = 51). p = 0.004. The p-value was determined by log-rank test. (E) Comparison of recurrence rate between patients with DSG2-high vs. DSG2-low tumors using chi-square test. p = 0.03. (F) Kaplan–Meier analysis of distant metastasis-free survival of patients with different levels of DSG2 using a breast cancer cohort (Yau 2010 dataset) from the UCSC Xena public hub. p = 0.008. The p-value was determined by log-rank test.

Figure 2. DSG2 expression promoted CTC clustering and metastatic colonization.

(A) Diagram of the procedure used for orthotopic xenografts. MDA-MB-231 cells expressing

EGFP without (MB231-EGFP shCtrl) or with DSG2 depletion (shDSG2) were injected into 4th mammary fat pads of NOD/SCIDγ mice. CTCs, primary tumors and lung tissues were collected at 9 weeks after injection. (B) Tumor weight of xenograft models using shCtrl and shDSG2 of EGFP-MDA-MB231 cells. Five mice were used for each group. All data are presented as mean ± SD (unpaired test) $^{**}p < 0.01$. (C) Representative H&E staining of lung sections from mice orthotopically injected with shCtrl or shDSG2 MDA-MB-231-EGFP cells. Quantification of lung nodule numbers between shCtrl and shDSG2 groups is shown. Four mice were used for each group. All data are presented as mean ± SD (unpaired test). (D) Representative IHC staining of DSG2 in lung nodules of the MDA-MB-231-EGFP shCtrl or shDSG2 tumor bearing mice. Scale bar, 100 μm. (E) Representative images of CTCs from shCtrl or shDSG2 MDA-MB-231-EGFP tumor bearing mice captured by the MiCareo on-chip filtration system. Positive immunofluorescence staining of EGFR, DSG2 and GFP identified MDA-MB-231-EGFP cells. (F) Numbers of single CTCs and CTC clusters collected from shCtrl or shDSG2 MDA-MB-231-EGFP tumor bearing mice.

Figure 3. DSG2 expression promoted metastatic colonization and tumor growth.

(A and C) Summary table of lung metastasis derived from tail vein injection using SKBR3 (A) and MDA-MB-157 (C) cells. (B and D) Analysis of lung nodule numbers between different groups. Right panel is representative hematoxylin and eosin (H&E) staining of lung sections from mice with

tail vein injection of DSG2-depleted SKBR3 (B) or DSG2-overexpressing MDA-MB-157 (D) cells. Scale bar, 100 μm. (E and F) Soft agar colony formation assays using DSG2-depleted MDA-MB-231 and SKBR3 cells (E) and DSG2-overexpressing MDA-MB-157 and MDA-MB-468 cells (F). The experiments were repeated three times. All data are presented as mean ± SD (unpaired test). $^{**}p < 0.01$. (G and H) Xenograft models using DSG2-depleted MDA-MB-231 and SKBR3 cells (G) and DSG2-overexpressing MDA-MB-157 and MDA-MB-468 cells (H) in NOD/SCIDγ mice. Five mice were used for each group.

Figure 4. DSG2 expression inhibited cell invasion, migration and intravasation.

(A and B) Wound-healing migration assays using DSG2-depleted MDA-MB-231cells (A) and DSG2-overexpressing MDA-MB-157 cells (B). (C and D) Transwell invasion assays using DSG2-depleted MDA-MB-231 and SKBR3 cells (C), and DSG2-overexpressing MDA-MB-157 and MDA-MB-468 cells (D). (E and F) FACS analysis of CTC numbers collected from mice 5 (E) or 8 (F) weeks after fat-pad injection between the control (black square) and DSG2-depleted (blue circle) groups analyzed by FACS. (G and H) IHC staining of DSG2 (G) and CAIX (H) using serial tumor sections from mice bearing MB231-EGFP shCtrl tumors. Enlarged images are presented on the right. Scale bar, 100 μm. (I) Representative IHC staining of DSG2 and CAIX using serial tumor sections from breast cancer patients. Enlarged images are presented on the right. Scale bar, 100

μm. The experiments were repeated at least twice. All data are presented as mean ± SD (unpaired test). *** $p < 0.001$, ** $p < 0.01$. * $p < 0.05$.

Figure 5. Hypoxia induced HIF1α-mediated DSG2 suppression via PRC2 complex.

(A) qRT-PCR analysis of DSG2 level in SKBR3 and MDA-MB-231 cells under normoxia or hypoxia for 16 hours. Cells under hypoxic stress are indicated by elevated HIF1α. GAPDH was used as an internal control. (B) Time-course IB of DSG2 and HIF1α in SKBR3 cells under normoxia or hypoxia. (C) qRT-PCR analysis of DSG2 level in HEK-293T cells transiently transfected with pcDNA vector or pcDNA-HIF1α-P564A plasmid. HIF1α expression was detected by IB. (D) qRT-PCR of DSG2 level in HEK-293T cells transduced with shHIF1α (clone # 675 and # 677) and treated with 100 μM CoCl2 for 24 hours. IB of HIF1α indicated that cells were under hypoxic stress. (E) Diagram shows three putative HIF1α binding sites predicted using ISMAR and the mutated sequences on the DSG2 promoter. Luciferase reporter assays using HEK-293T cells co-transfected with pcDNA.HIF1α and the wild type (Wt) or mutant DSG2 promoter constructs. (F) ChIP-qPCR analysis of HIF1α on the P2 region (containing -946~-943 nt upstream of TTS) in SKBR3 cells under normoxia or hypoxia for 8 hours. (G) ChIP-qPCR analysis of EZH2, SUZ12 and H3K27me3 on the P2 region in SKBR3 cells under normoxia or hypoxia for 8 hours. The experiments were repeated three times independently. All data are presented as mean ± SD (unpaired

test). *** $p < 0.001$, **$p < 0.01$. *$p < 0.05$. (H) qRT-PCR analysis of DSG2 level in SKBR3 cells under normoxia or hypoxia. Black circle indicates cells under normoxia throughout the experiment. Gray triangle indicates cells under hypoxia for 8 hr and then released from the stress for 28 hr. Red square indicates cells under hypoxia throughout the experiment. (I) FACS analyses to examine DSG2 levels in CTCs disseminated from orthotopically metastatic mouse derived from EGFP-MDA-MB231 cells 9 weeks after injection.

Figure 6. Diagram illustrating how dynamic changes of DSG2 expression contribute to breast tumorigenesis and metastasis. High DSG2 expression promotes breast tumor growth in mammary tissue. When the tumor is large enough to induce hypoxia, HIF1α is stabilized and recruits PRC2 complex (EZH2 and SUZ12) to the DSG2 promoter to suppress its transcription. DSG2 suppression allows EMT, invasion and intravasation to occur. In circulatory system, hypoxic stress is released and DSG2 expression is reactivated which allows CTC clustering in blood and colonization in lung.

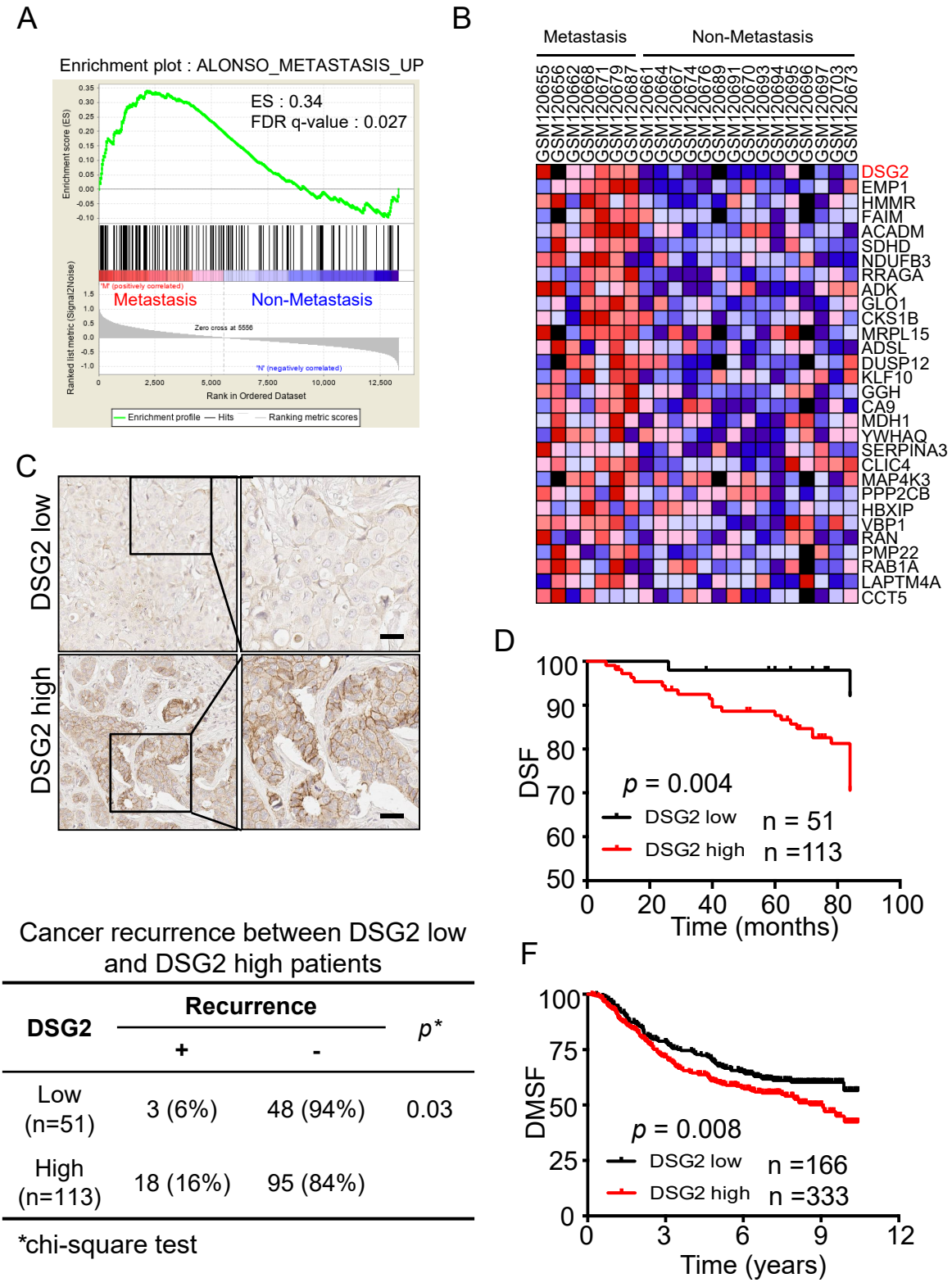

E

Cancer recurrence between DSG2 low and DSG2 high patients

DSG2	Recurrence		p*
	+	-	
Low (n=51)	3 (6%)	48 (94%)	0.03
High (n=113)	18 (16%)	95 (84%)	

*chi-square test

Figure 1

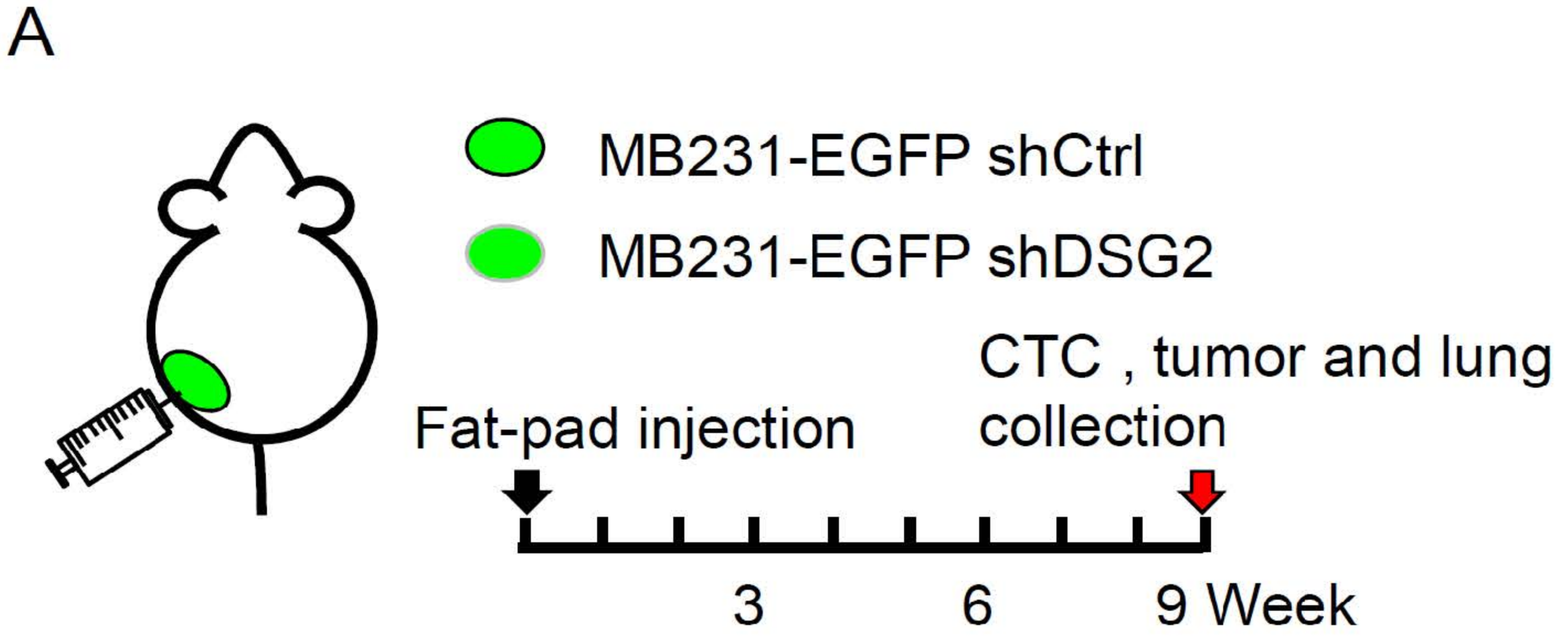

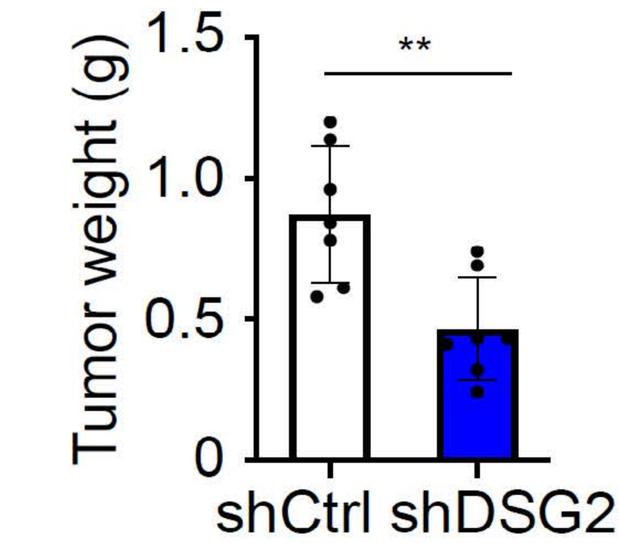

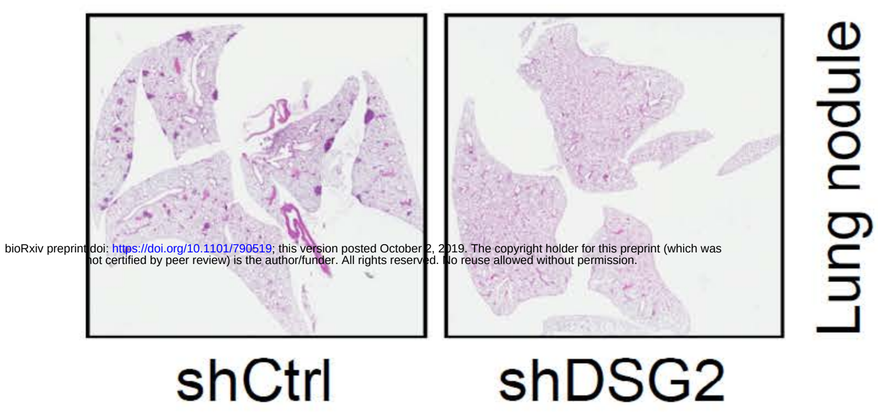

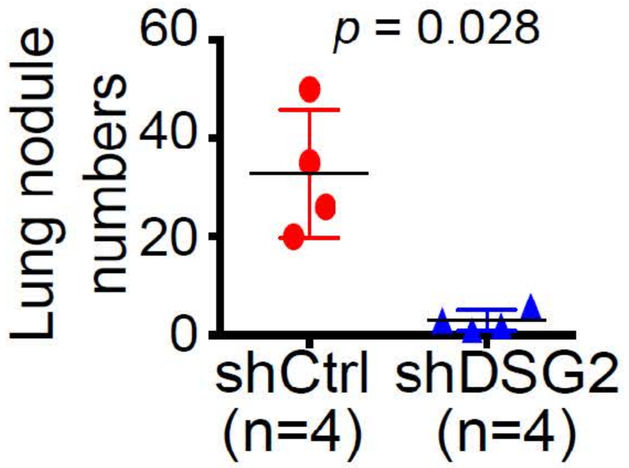

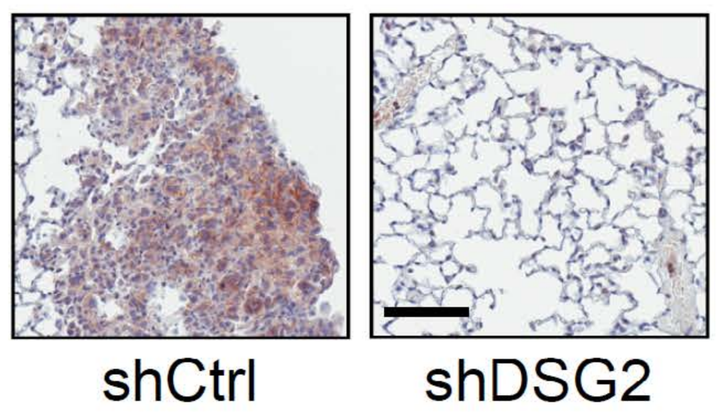

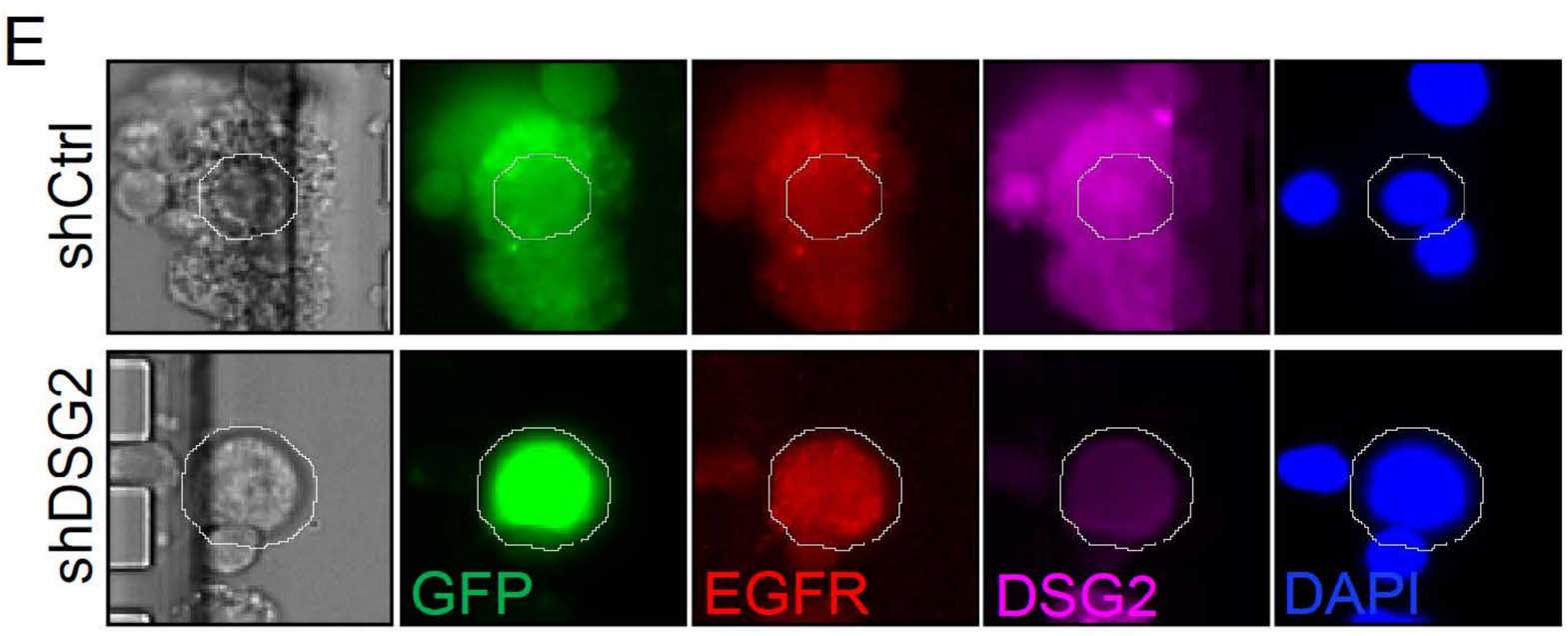

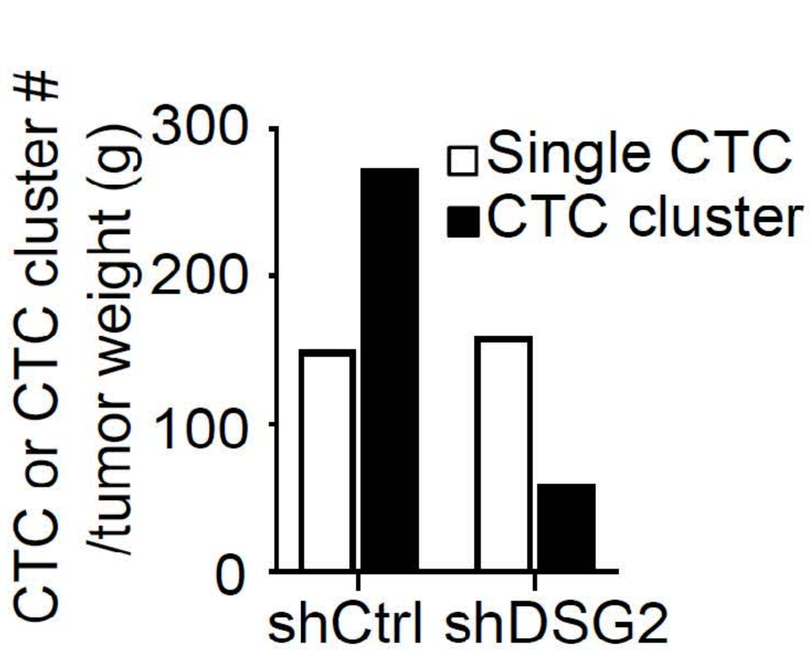

Figure 2

A

Tail vein injection with SKBR3 cells

	Lung colonization
shCtrl	7/7 (100%)
shDSG2	2/7 (28%)

C

Tail vein injection with MB157 cells

	Lung colonization
Ctrl	1/10 (10%)
DSG2 oe	9/10 (90%)

B

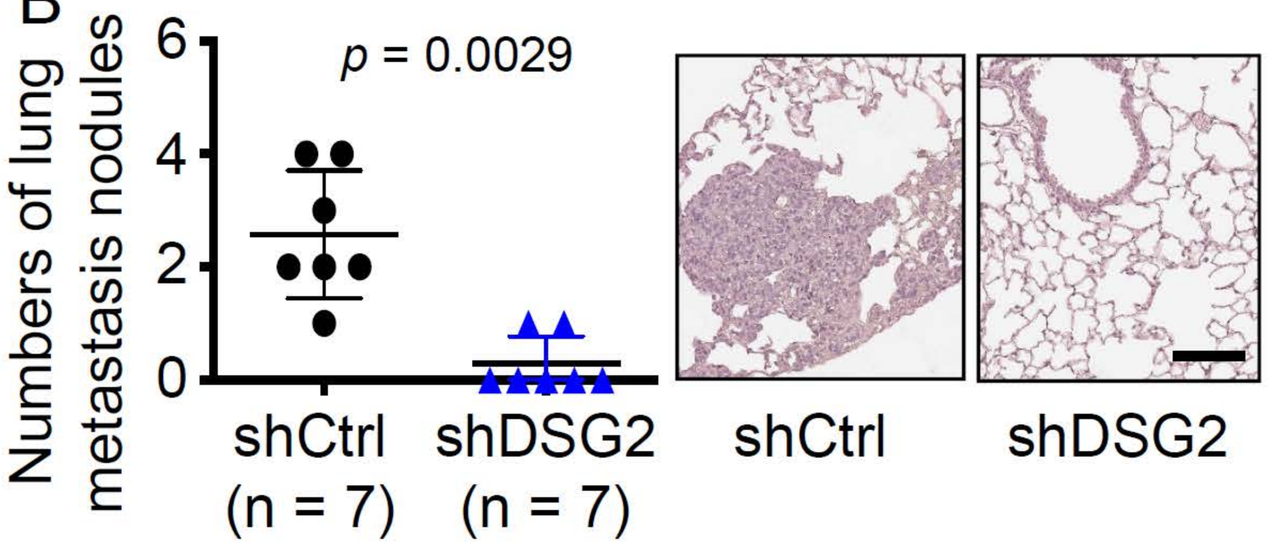

D

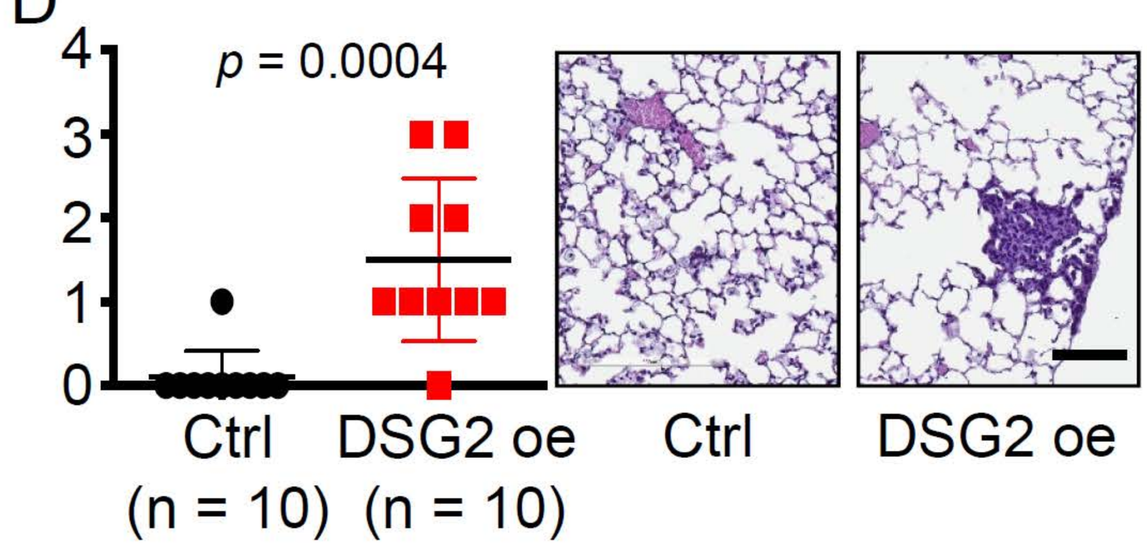

E

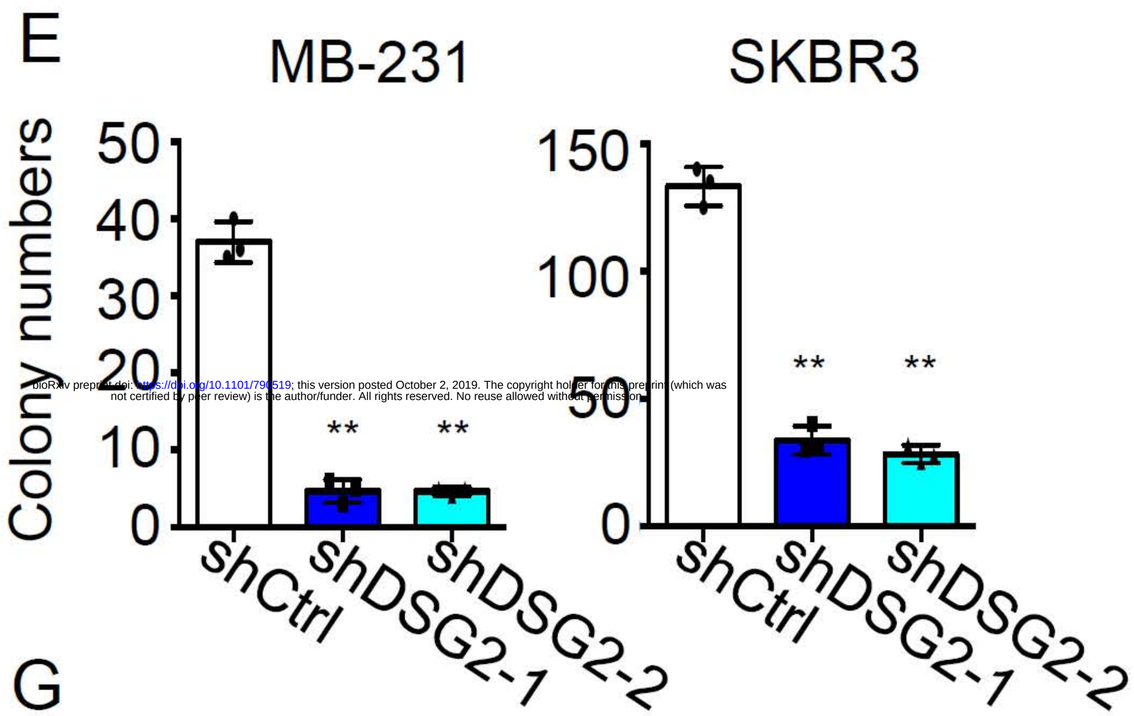

F

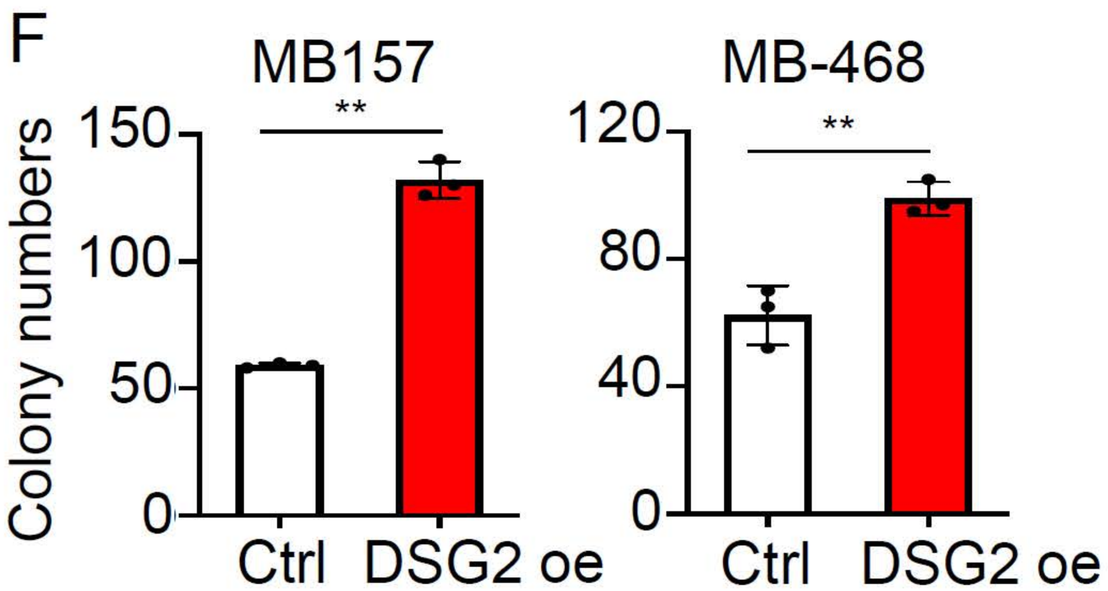

G

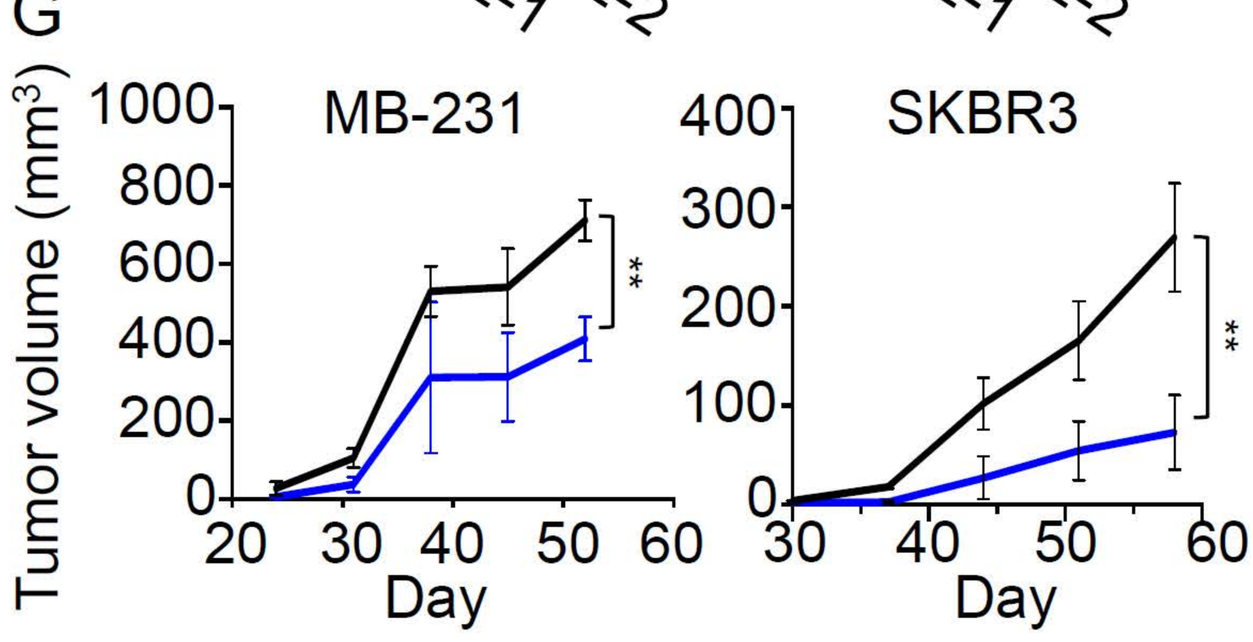

H

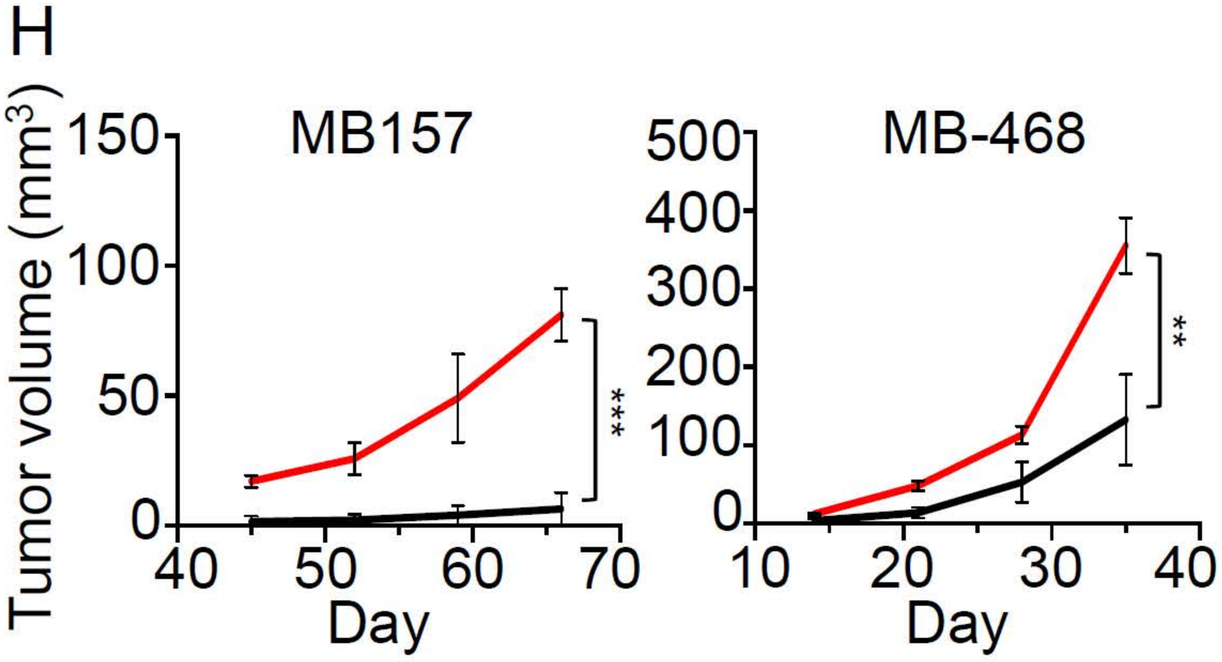

Figure 3

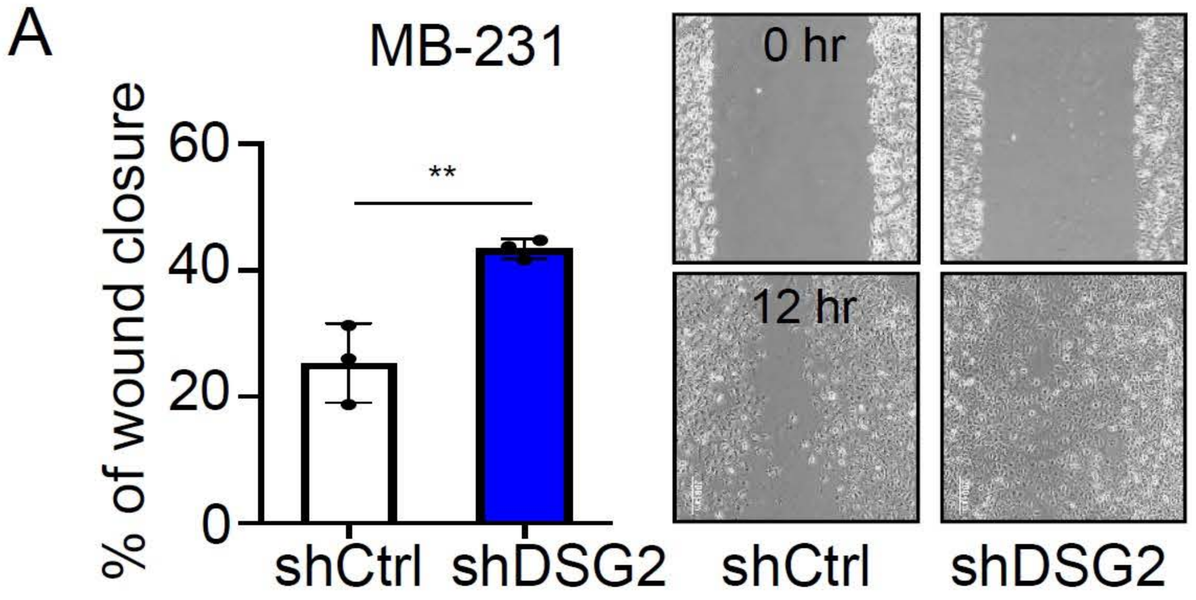

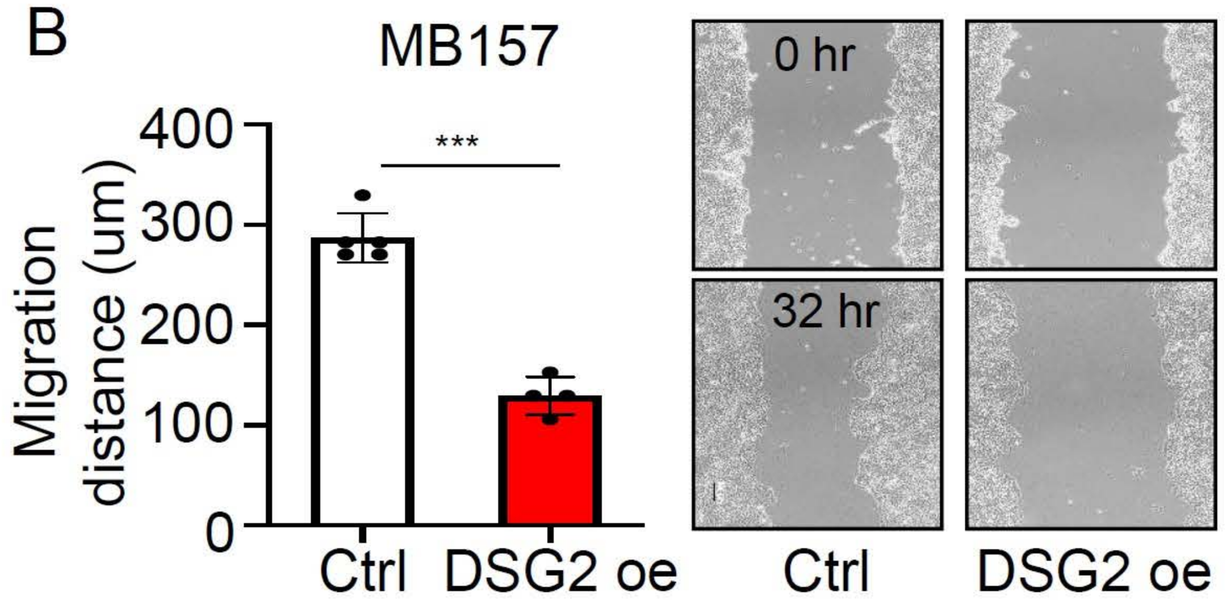

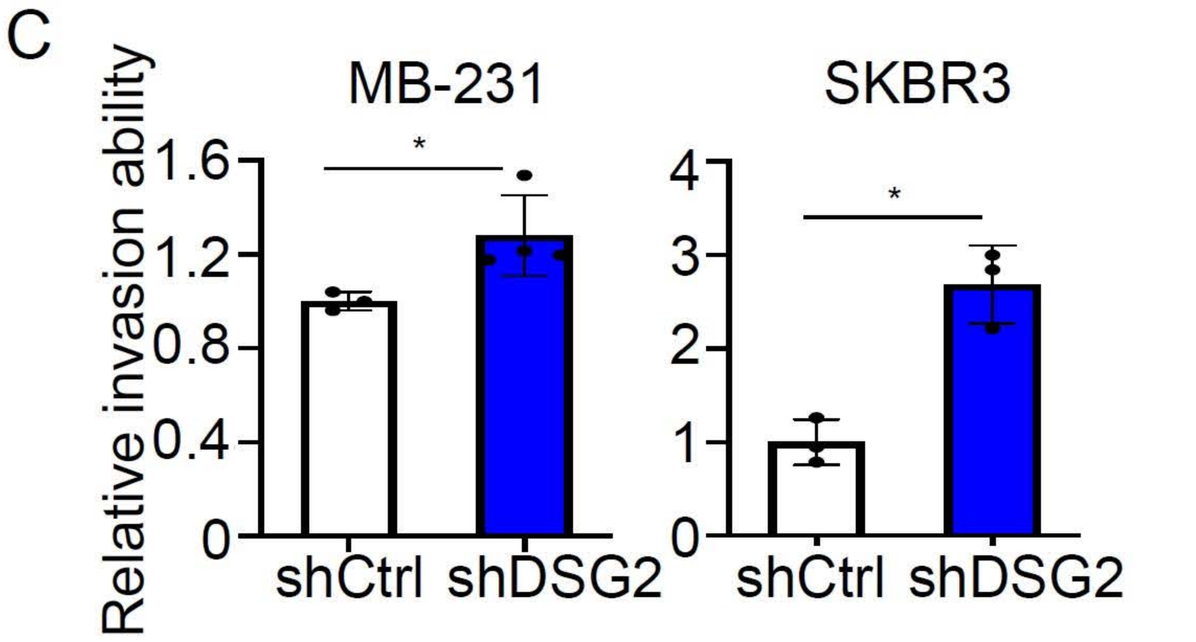

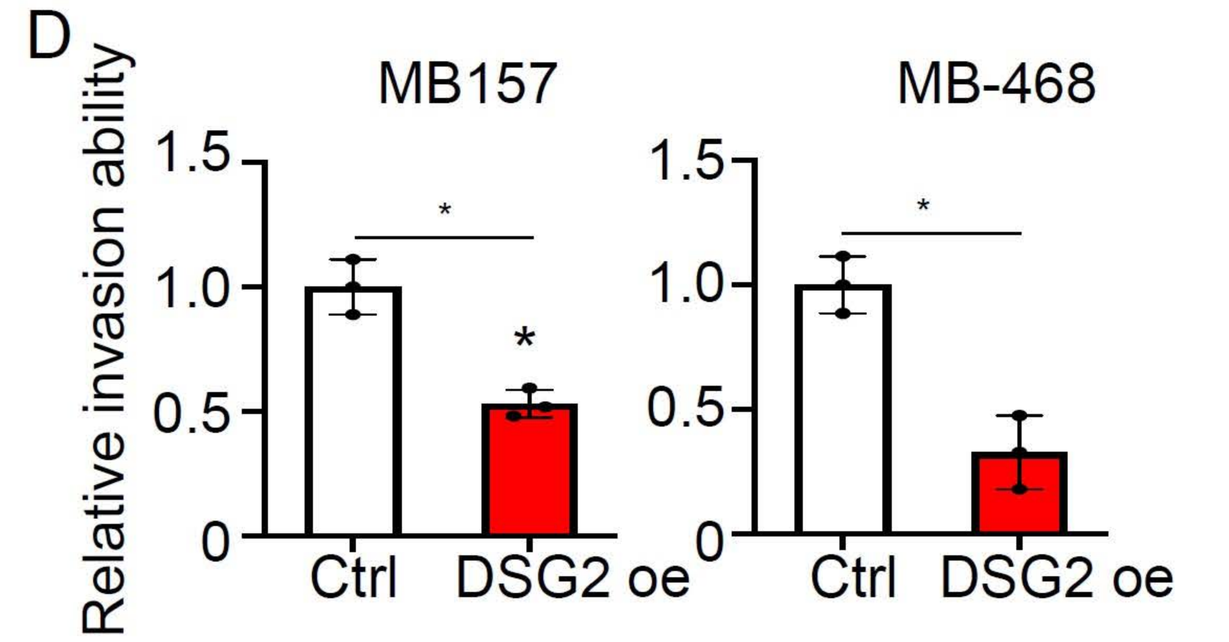

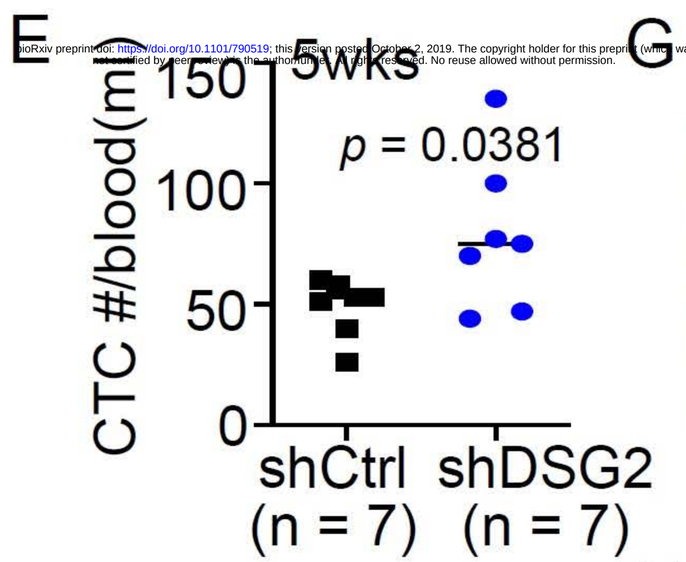

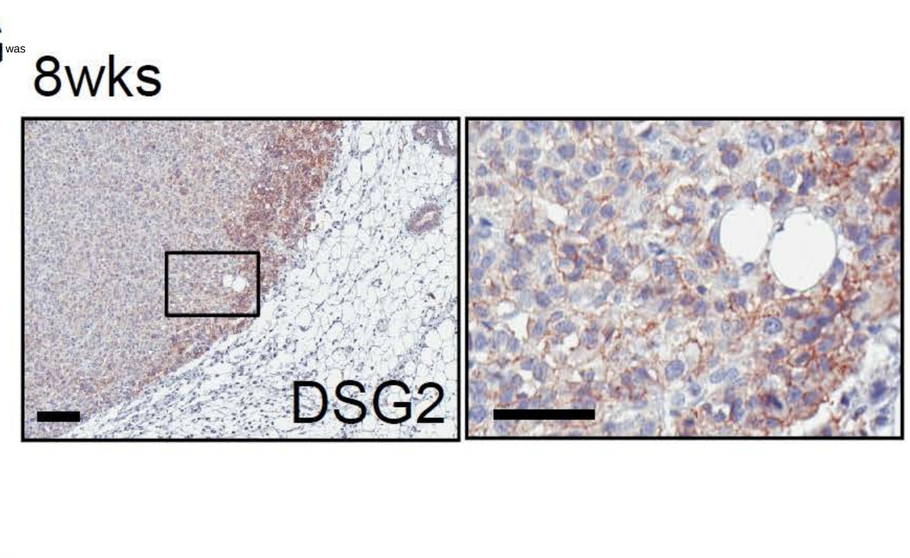

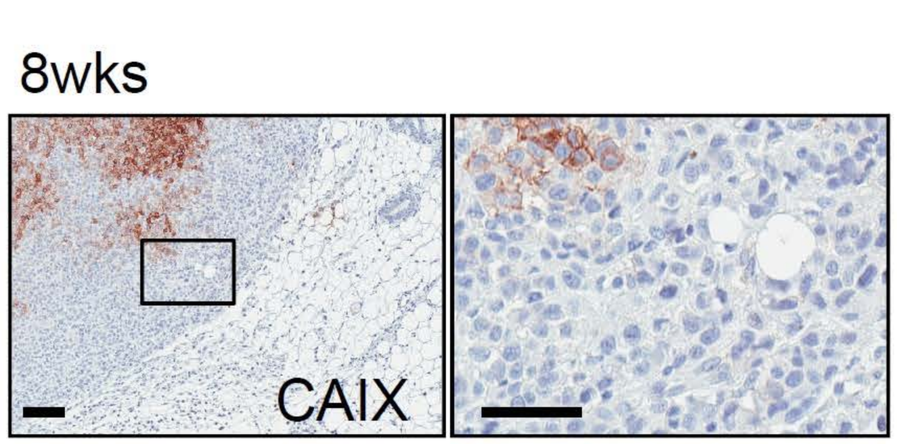

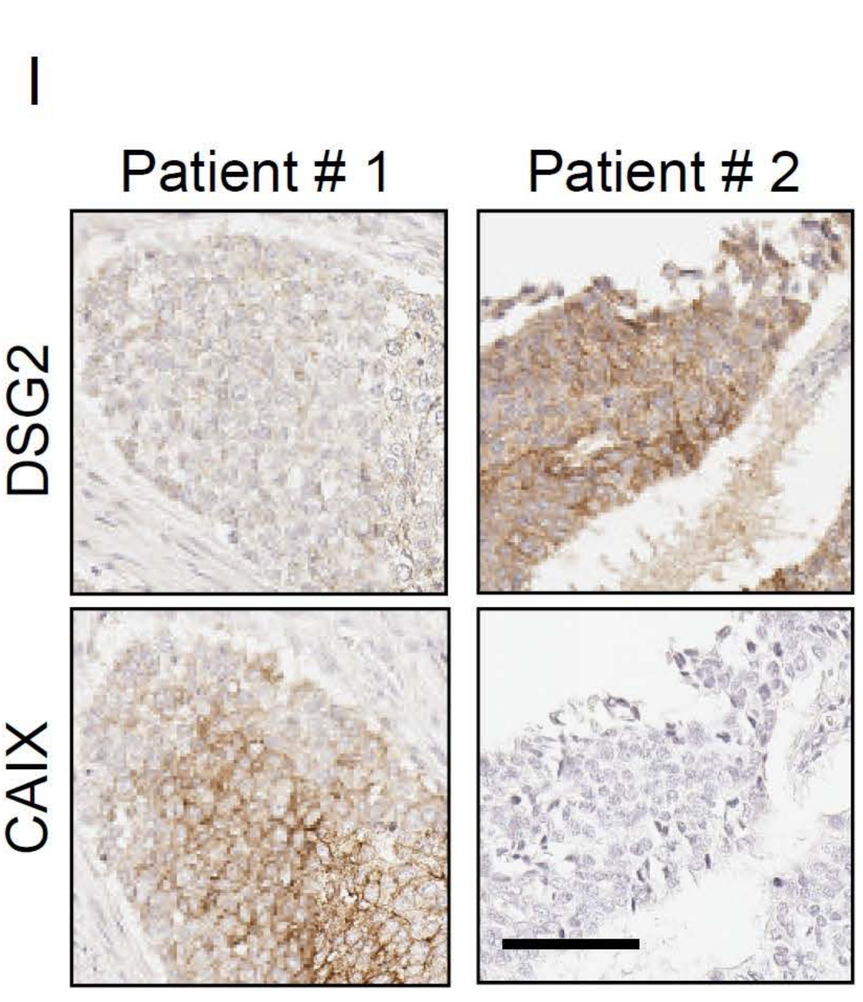

Figure 4

Figure 5

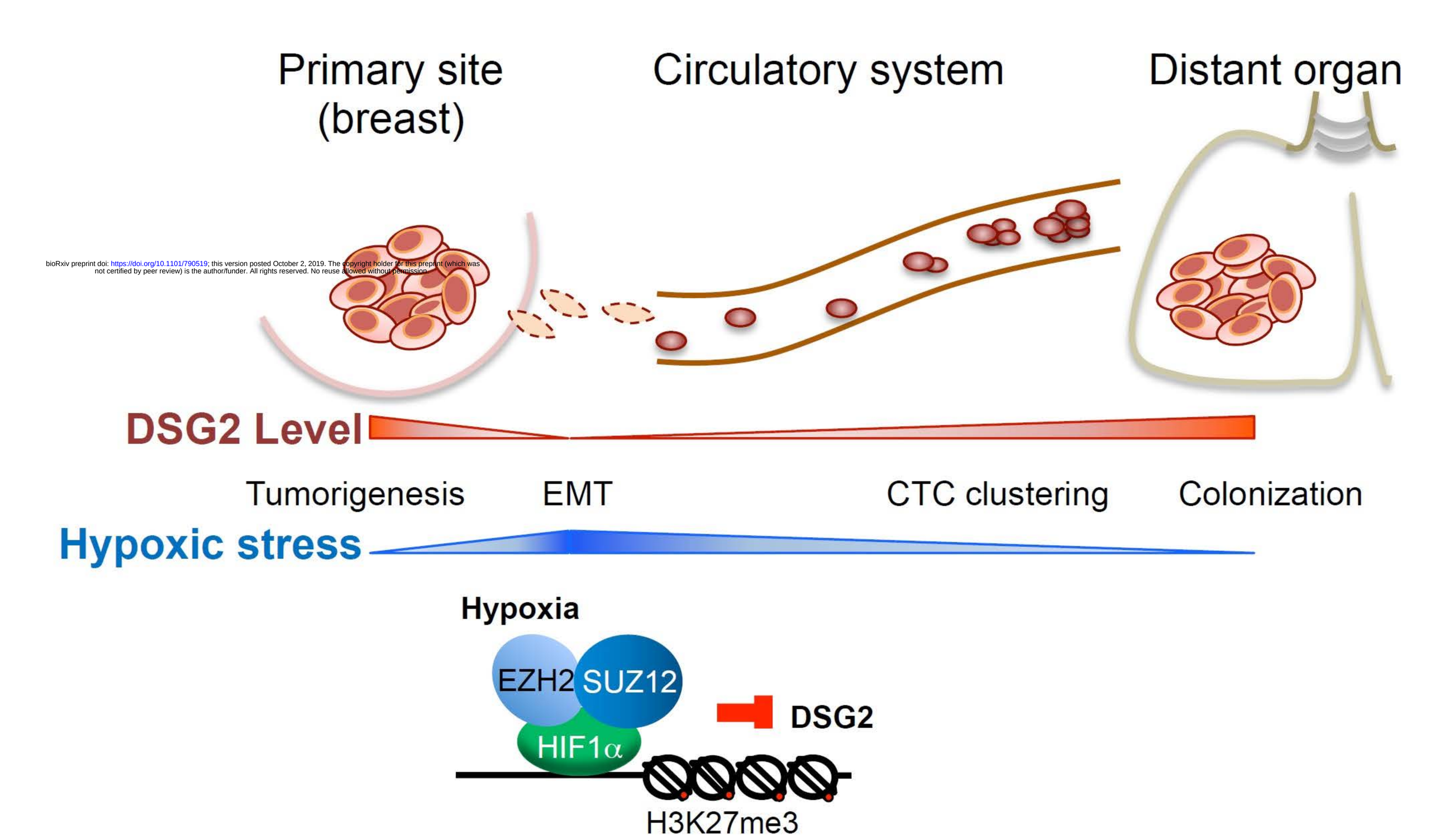

Figure 6